Journal of Experimental Pharmacology

Dovepress
open access to scientific and medical research

Open Access Full Text Article

ORIGINAL RESEARCH

Pharmacological Activities of Fingerroot Extract and Its Phytoconstituents Against SARS-CoV-2 Infection in Golden Syrian Hamsters

Teetat Kongratanapasert[1,*], Supasek Kongsomros[2,5,*], Nlin Arya[3], Kripitch Sutummaporn[3], Witthawat Wiriyarat[3], Yada Akkhawattanangkul[4], Tussapon Boonyarattanasoonthorn[5], Nithi Asavapanumas[5], Phongthon Kanjanasirirat[6], Ampa Suksatu[2], Khanit Sa-ngiamsuntorn[7], Suparerk Borwornpinyo[6,8], Pornpun Vivithanaporn[5], Somchai Chutipongtanate[5,9], Suradej Hongeng[6,9], Boonsong Ongphiphadhanakul[10], Arunee Thitithanyanont[2], Phisit Khemawoot[5], Piyamitr Sritara[10]

[1]Program in Translational Medicine, Faculty of Medicine Ramathibodi Hospital, Mahidol University, Bangkok, 10400, Thailand; [2]Department of Microbiology, Faculty of Science, Mahidol University, Bangkok, Thailand; [3]Department of Preclinic and Applied Animal Science, Faculty of Veterinary Science, Mahidol University, Nakhonpathom, 73170, Thailand; [4]Department of Clinical Medicine and Public Health, Faculty of Veterinary Science, Mahidol University, Nakhonpathom, 73170, Thailand; [5]Chakri Naruebodindra Medical Institute, Faculty of Medicine Ramathibodi Hospital, Mahidol University, Samutprakarn, 10540, Thailand; [6]Excellence Center for Drug Discovery, Faculty of Science, Mahidol University, Bangkok, 10400, Thailand; [7]Department of Biochemistry, Faculty of Pharmacy, Mahidol University, Bangkok, 10400, Thailand; [8]Department of Biotechnology, Faculty of Science, Mahidol University, Bangkok, 10400, Thailand; [9]Department of Pediatrics, Faculty of Medicine Ramathibodi Hospital, Mahidol University, Bangkok, 10400, Thailand; [10]Department of Medicine, Faculty of Medicine Ramathibodi Hospital, Mahidol University, Bangkok, 10400, Thailand

*These authors contributed equally to this work

Correspondence: Phisit Khemawoot, Chakri Naruebodindra Medical Institute, Faculty of Medicine Ramathibodi Hospital, Mahidol University, Bang Phli, Samut Prakarn, 10540, Thailand, Tel/Fax +66 28395161, Email phisit.khe@mahidol.ac.th

Background: The outbreak of COVID-19 has led to the suffering of people around the world, with an inaccessibility of specific and effective medication. Fingerroot extract, which showed in vitro anti-SARS-CoV-2 activity, could alleviate the deficiency of antivirals and reduce the burden of health systems.

Aim of Study: In this study, we conducted an experiment in SARS-CoV-2-infected hamsters to determine the efficacy of fingerroot extract in vivo.

Materials and Methods: The infected hamsters were orally administered with vehicle control, fingerroot extract 300 or 1000 mg/kg, or favipiravir 1000 mg/kg at 48 h post-infection for 7 consecutive days. The hamsters (n = 12 each group) were sacrificed at day 2, 4 and 8 post-infection to collect the plasma and lung tissues for analyses of viral output, lung histology and lung concentration of panduratin A.

Results: All animals in treatment groups reported no death, while one hamster in the control group died on day 3 post-infection. All treatments significantly reduced lung pathophysiology and inflammatory mediators, PGE_2 and IL-6, compared to the control group. High levels of panduratin A were found in both the plasma and lung of infected animals.

Conclusion: Fingerroot extract was shown to be a potential of reducing lung inflammation and cytokines in hamsters. Further studies of the full pharmacokinetics and toxicity are required before entering into clinical development.

Keywords: *Boesenbergia rotunda*, Zingiberaceae, panduratin A, SARS-CoV-2, COVID-19, hamster

Introduction

The world has been confronted with an emerging infectious disease, coronavirus disease 2019 (COVID-19), which is caused by severe acute respiratory syndrome coronavirus 2 (SARS-CoV-2).[1] According to the Centre for Systems Science and Engineering, over 500 million people around the world have been infected, with 6 million deaths, as of July 13, 2022. Symptoms of COVID-19 cases vary among individuals,[2] and some patients have developed severe pneumonia and pulmonary infiltrates that could cause a reduction of oxygen saturation, respiratory failure and, ultimately,

Received: 22 July 2022
Accepted: 24 December 2022
Published: 19 January 2023

death.[3] Currently, the COVID-19 treatment guidelines recommended the use of a combination of antivirals and corticosteroids in hospitalized patients.[4,5] The efficacy of dexamethasone, a corticosteroid drug, is already been confirmed by the decreasing mortality in severe or critical COVID-19 cases.[6] However, antiviral drugs, eg, remdesivir and favipiravir show a significant benefit only in non-hospitalized cases.[7] Data from interim analysis of MOVe-IN study showed that molnupiravir failed to benefit hospitalized patients, but could reduce the risk of hospitalization and death of non-hospitalized patients in MOVe-OUT study.[8] Another drug, PAXLOVID, can reduce the risk of hospitalization and death of non-hospitalized patients at high risk of severe progression in EPIC-HR study.[9] Nonetheless, there are no highly effective antiviral drugs for hospitalized patients. Various types of COVID-19 vaccines have already been launched, with various limitations, eg, accessibility, availability, efficacy; meanwhile, virus mutations might cause breakthrough infections in immunized individuals. Therefore, the development of medicines for COVID-19 treatment is required in parallel with vaccinations, to minimize the outbreak.[10]

In the need for antivirals, approved drugs and natural products are screened in order to evaluate the antiviral activity. Natural products are considered to be a potential source for drug discovery for cancer and infectious diseases.[11] Previously, our team has screened 114 Thai medicinal plant extracts and several purified compounds, and found that *Andrographis paniculata* extract and its major bioactive component, andrographolide, exhibited anti-SARS-CoV-2 activity in Calu-3 cells, with an IC_{50} of 0.036 μg/mL and 0.034 μM, respectively.[12] Meanwhile, *Boesenbergia rotunda* or fingerroot and its phytochemical component, panduratin A, have anti-SARS-CoV-2 activity in Vero E6 cells, with an IC_{50} of 3.62 μg/mL and 0.81 μM, respectively, compared with remdesivir which has an IC_{50} of 2.71 μM.[13] With this potential, we selected *B. rotunda* extract for further development, since *A. paniculata* was commercially available and approved for COVID-19 treatment in Thailand already. Further investigations of the efficacy, toxicity and pharmacokinetics of fingerroot extract in animal models are urgently needed for phytopharmaceutical product development against the viral outbreaks. The golden Syrian hamster (*Mesocricetus auratus*) is a suitable model to determine antiviral activity in an animal experiment, since it is known that the virus primarily targets the ACE2 receptor on epithelial cells of the upper respiratory tract and alveolar type II cells of the lung.[3,14] The respiratory organ of the hamster has ACE2 receptors and can be infected via the intranasal route, resulting in mild-to-moderate disease and pathological lesions in the lung that are similar to humans.[15]

Boesenbergia rotunda (L.) Mansf., or fingerroot, is a tropical plant from the Zingiberaceae family (Figure 1A), mostly found in Southeast Asia, South Asia and Southern China.[16] The major chemical constituents of *B. rotunda* are flavonoids (eg, geraniol, krachaizin, panduratin, pinostrobin and pinocembrin), essential oils (eg, nerol, camphor, cineole, fenchene and hemanthidine) and polyphenols (eg, coumaric acid, chlorogenic acid, hesperidin, kaempferol, naringin and quercetin).[17] Panduratin A is one of the major phytochemicals in fingerroot, with physicochemical properties including water solubility of 0.0003191 mg/L at 25°C, a partition coefficient of XLogP3-AA = 6, and a molecular weight of 406.5 g/mol.[18] Fingerroot and panduratin A possess several activities, eg, antimicrobial, antioxidant, antiulcer, antimutagenic, anticancer and anti-inflammatory.[16] Among these, there are reports that panduratin A inhibited HIV-1 protease, with an IC_{50} of 18.7 μM, and also demonstrated potent inhibitory activity against nitric oxide (NO) and anti-prostaglandin E2

Figure 1 Physical appearance of (**A**) the fingerroot whole plant, (**B**) rhizome, and (**C**) fingerroot extract.

(PGE_2), with IC_{50} values of 0.175 and 0.0195 μM, respectively.[19,20] In addition, fingerroot could decrease interleukin-6 (IL-6) plasma level in ulcer rats.[21] Proteomics analysis of COVID-19 patients showed an association between the plasma level of IL-6 and severity of the disease, which indicated IL-6 as biomarker for COVID-19 severity.[22] Interestingly, fingerroot possesses both anti-SARS-CoV-2 and anti-inflammatory activities in vitro. These features might be beneficial for COVID-19 treatment, in terms of the antiviral and anti-inflammatory activities. Therefore, this research aims to evaluate the safety and efficacy of fingerroot extract against SARS-CoV-2-infection in hamsters. Animal tolerability, panduratin A concentration in plasma and lung, viral reduction in lung, reduction of lung inflammation, and cytokine levels were determined for further clinical development of fingerroot extract.

Materials and Methods

Cell Line and Virus

Vero E6 cell, African green monkey (*Cercopithecus aethiops*) kidney epithelial cells, was obtained from American Type Culture Collection (ATCC, USA). Cells were cultured in Dulbecco's modified Eagle medium (DMEM) (Gibco, USA) with 10% FBS (Gibco, USA), 100 U/mL penicillin, and 100 μg/mL streptomycin (Gibco, USA). SARS-CoV-2 (SARSCoV-2/human/THA/LJ07_P3/2020) was isolated from nasopharyngeal swabs of a confirmed COVID-19 patient in Thailand. The consensus sequences of the spike protein of the wild type have been deposited in GenBank and can be accessed under the accession numbers SARSCoV-2/human/THA/LJ07_P3/2020.[10] Viral stocks were propagated in Vero E6 cells. Briefly, the virus was adsorbed onto a monolayer of Vero E6 cells at 37°C for 1 h. SARS-CoV-2 infected cells were washed, and the infection media was replaced with 2% fetal bovine serum (FBS) in Dulbecco's modified Eagle's medium (DMEM) with 100 U/mL penicillin and 100 μg/mL streptomycin (Gibco, USA). Infected cells were incubated at 37°C with 5% CO_2. The supernatant, containing the virus, was collected at day 4 post infection. Viral titers were determined by plaque assay. The virus was propagated in Vero E6 cells by two passages to establish a high-titre stock (passage 3). All procedures involving SARS-CoV-2 were performed in a certified Biosafety level 3 laboratory at the Department of Microbiology, Faculty of Science, Mahidol University, Thailand.

Plant Material and Test Compounds

The rhizome of *Boesenbergia rotunda* (L). Mansf. was collected from Pathum Thani, Thailand, in 2020 (Figure 1B). A voucher specimen (S. Ruchisansakun 1981 (SLR)) was deposited at Talaad Thai, Pathum Thani, Thailand, after identification by Assistant Professor Dr Saroj Ruchisansakun. Fingerroot extract (a dark brown viscous liquid with characteristic odor) containing panduratin A 9.6% w/w (Figure 1C), as determined by LC-MS analysis, was provided by the Excellence Centre for Drug Discovery, Thailand. Herbal extraction and preparation was described previously.[13] Favipiravir was kindly provided by the Ministry of Public Health, Thailand. Dimethyl sulfoxide (DMSO) was purchased from Merck, Germany. Panduratin A standard reference was purchased from Biosynth Carbosynth, United Kingdom, with ≥98% purity.

Animal Experiment

Ethical approval: all animal experiments were approved by the Faculty of Veterinary Science, Mahidol University-Institute Animal Care and Use Committee (approval no. MUVS-2020-07-26; approval date Oct 01, 2020) and were performed in compliance with the ethical principles and guidelines for the use of animals.[23] The ARRIVE guidelines were followed for the reporting of animal experiments. All procedures involving SARS-CoV-2 were performed in a certified animal biosafety level 3 laboratory at the Faculty of Veterinary Science, Mahidol University, Thailand. Replacement: hamsters were used, as a least sentient animal model for SARS-CoV-2 study. Reduction: sample sizes were calculated for minimal samples, using, $N = 2 \times SD^2 \times (Z_{\alpha/2} + Z_{\beta})^2/d^2$, with SD being the standard deviation (50%), $Z_{\alpha/2}$ being the confidence level (95% confidence interval), Z_{β} being the power level (80% power) and d being the statistical significance (100%). From the equation, the sample size was 4 hamsters per subgroup, or 12 hamsters per group. Refinement: all animal procedures were conducted according to animal work standard operating procedures and

following best practices regarding animal handling, treatment and care. Hamsters were anesthetized during inoculation and euthanasia. A humane endpoint was planned when animals have lost more than 15% of their weight.[24]

Eight-week-old male Crl:LVG(SYR) hamsters were purchased from Beijing Vital River Laboratory Animal Technology, China, then quarantined and acclimatized for 2–3 weeks. Four hamsters were caged in static filter top cages with sterile corncob, in a specific pathogen-free room, and health conditions were monitored before beginning the experiment. Animals were fed *ad libitum* and were kept in an environmental control at 20–25°C, 50–70% humidity and 12:12 h light/dark cycle. Animals were observed for appearance, behavior and activity on a daily basis and were weighed every week to determine their health status. A total of 48 hamsters were randomly divided into four groups. At day 0, all hamsters of each group were intranasally infected with 50 µL of culture medium DMEM with 2% FBS containing 3.75×10^4 PFU of SARS-CoV-2 (n = 12 per treatment group, n = 4 per subgroup, sacrificed at day 2, 4 and 8 post-infection). Confirmation of infection was conducted by monitoring appearance, behavior and activity at day 1 post-infection. At day 2 post-infection, a control (50% DMSO) or treatment (300 or 1000 mg/kg fingerroot extract, or 1000 mg/kg favipiravir as standard treatment prepared in 50% DMSO) were orally administered for 7 consecutive days.

At day 2, 4 and 8 post-infection, after dosing the test compound for 4 h, four hamsters of each subgroup were deeply anesthetized with isoflurane inhalation for exsanguination, and then euthanized with an isoflurane overdose (30–40%) using the open-drop technique. Blood and lungs were collected by cardiac puncture and necropsy, respectively. All animal procedures were performed in a biosafety cabinet class II.

Plaque Assay

A confluent monolayer of Vero cells was inoculated with a series of ten-fold dilutions of SARS-CoV-2 virus for 1 h. After incubation, the supernatant was removed and overlaid with a plaque assay medium containing 1.2% Avicel (RC581; FMC BioPolymer, USA), 2% FBS with 100 U/mL penicillin and 100 µg/mL streptomycin (Gibco, USA). The plaque was incubated at 37°C for 72 h. Thereafter, the monolayer was fixed with 3.7% formaldehyde for 1 h, and the cell monolayer was stained with 1.25% crystal violet. The plaque forming unit per milliliter (PFU/mL) was calculated.

Viral Quantification by qRT-PCR and Focus Forming Assay

Lung tissues were weighed and homogenized using a BeadBug bead homogenizer (Benchmark Scientific, USA) with 1.0 mm of zirconia beads (BioSpec Products, USA) in 1 mL of iced-cold DMEM media at 4000 rpm for 2 min. The tissues were then clarified by centrifugation at 6000 rpm for 3 min. Supernatant was transferred to a 2 mL tube for further measurement of viral load. All experiments involving hamster infection were performed in an animal biosafety level 3 laboratory at the Faculty of Veterinary Science, Mahidol University, Thailand.

The total RNA was extracted from 250 µL of homogenized lung tissues (~25 mg of tissue) using an RNeasy plus Mini kit (Qiagen, Germany). The RT-qPCR assays were performed in a final volume of 20 µL using a QIAGEN OneStep RT-PCR kit (Qiagen, Germany). A known number of SARS-CoV-2 RNA copies were used for the generation of a standard curve to determine the absolute quantity of the viral load in the homogenized tissues. The following primers were used: Spike forward (5'- CCT ACT AAA TTA AAT GAT CTC TGC TTT ACT-3'); Spike reverse (5'- CAA GCT ATA ACG CAG CCT GTA −3') Thermal cycling conditions were as follows: 50°C for 30 min, 95°C for 15 min, followed by 40 cycles at 95°C for 30s, 55°C for 30s and 72°C for 60s. The RT-qPCR assays were tested on the Rotor-Gene Q qPCR system (QIAGEN, Germany). Analysis of the copy numbers and linear regression curve was performed using the software Rotor Gene Q (QIAGEN, Germany).

The infectious SARS-CoV-2 titers were determined by the focus forming assay (FFA) in Vero E6 cells. First of all, 10-fold serially diluted tissue supernatants were inoculated to Vero-E6 cell in 96-well plates for 1 h. The inoculum was removed carefully, and the cell monolayer was overlaid with 2% FBS in DMEM medium containing 1.2% Avicel (RC581; FMC BioPolymer, USA) with 100 U/mL penicillin and 100 U/mL streptomycin (Gibco, USA), before being placed at 37°C, 5% CO_2 for 24 h. The overlay medium was removed carefully, and the cell monolayer was fixed with 4% formaldehyde in PBS (phosphate buffered saline) for 1 h and then washed three times with PBS. To detect the viral foci, cells were permeabilized in 0.5% triton X-100 at room temperature for 10 min, then washed twice with PBS, and incubated with 1:2500 rabbit monoclonal antibody against SARS-CoV-2 Nucleoprotein (Sino Biological, China) at room

temperature for 1 h. Cells were then washed three times with PBS, incubated with 1:1000 horseradish peroxidase-conjugated goat anti-rabbit IgG secondary antibody (DAKO, USA) and stained with True-Blue peroxidase substrate (Sera Care, USA). Viral Foci were counted, and the viral load in the homogenized tissues was calculated as focus forming units (FFU) per gram of tissue.

Pharmacokinetic Analysis of Panduratin A

Lung tissues were harvested and stored in pre-weighed tubes containing 1.0 mm of zirconia beads (BioSpec Products, USA). Tissues were weighed and homogenized using a BeadBug bead homogenizer (Benchmark Scientific, USA) with zirconia beads, at 4000 rpm for 2 min. The mixtures were then centrifuged at 5000 × g for 5 min. Supernatant was transferred to a 1.7-mL tube and stored at −20°C. Blood was harvested and centrifuged at 5000 × g for 5 min, and the plasma was then collected and stored at −20°C.

The quantification of panduratin A in plasma and lung tissue was performed by a validated liquid chromatography tandem mass spectrometry (Shimadzu, Japan) equipped with a C18 reversed phase column and with a Guard C18 column (Phenomenex, USA). The column oven was maintained at 40°C and operated using a mobile phase consisting of 0.2% formic acid in water (solvent A) and 100% methanol (solvent B), with a gradient system (0–0.5 min 10% B, 0.5–1.5 min increase to 90% B, 1.5–2.5 min 90% B, 2.5–3.5 min decrease to 10% B, 3.5–4.5 min 10% B), at a flow rate of 0.5 mL/min and 10 µL injection volume. The mass spectrometer was a triple quadrupole with negative mode electrospray ionization. The mass-to-charge ratio of the panduratin A was 405.10/165.90 Da. The accuracy, precision, recovery and stability of the three quality control samples (10, 150 and 600 µg/L) were within acceptable limits. The lower limit of quantification was 1.22 µg/L (Supplementary Figure S1 and Supplementary Table S1). The calibration curves were in the range of 10–1000 µg/L. When the concentration of the samples exceeds the linear calibration curve, blank matrices were used to dilute the sample before protein precipitation. All samples were processed by simple protein precipitation, adding 200 µL of methanol into 50 µL of sample matrix and vortex mixing for 10 min. The mixtures were centrifuged at 12,000 × g at 4°C for 10 min, and the supernatant was transferred into a vial for LC-MS analysis. All the operations, acquisition and analysis of data were controlled by LabSolution software, version 5.86 (Shimadzu, Japan).

Histopathology

Lung specimens were collected from hamsters in each group. All lung samples were fixed in 10% neutral buffered formalin, cut in the midsagittal plane, dehydrated in 98% ethanol and embedded in paraffin as formalin-fixed paraffin-embedded (FFPE) lung tissues for pathological evaluation and detection of viral antigens. The FFPE lung samples were sectioned at 3 µm and deparaffinised with xylene, rehydrated with absolute ethanol and stained with haematoxylin and eosin (H&E). For evaluation of the H&E sections, the pathological findings were observed for microscopic diagnosis and evaluated for severity of lung lesions by experienced veterinary pathologists in a blind manner.

Immunohistochemistry for SARS-CoV-2 Viral Antigen Detection

For immunohistochemistry (IHC), the FFPE lung tissues were sectioned at 6 µm, deparaffinised and rehydrated for staining preparation. The sections were then incubated in antigen unmasking solution vector (pH 6) at 95°C for 45 min for antigen retrieval. The endogenous tissue peroxidase was inactivated by 3% H_2O_2 at room temperature for 10 min, washed with washing buffer (Dako, USA), and digested with 20 µg/mL Proteinase K for 5 min at 37°C. To block non-specific reactions, the sections were incubated with 5% BSA (Sigma-Aldrich, USA) for 30 min. The sections were incubated with 1:400 dilutions of the SARS-CoV-2 Nucleoprotein/NP antibody, Rabbit Mab, Cat. No, 40143-R001 diluted in blocking buffer for 1 h at 37°C in a moist chamber. After washing with PBS, the sections were incubated with 1:25 polyclonal goat anti-rabbit immunoglobulin/AP secondary antibody, code No. D0487 diluted with blocking buffer for 1 h at 37°C in a moist chamber. The antibody was labelled with liquid permanent red (Dako, USA), and the signal was developed in LPR chromogen and substrate buffer for 20 min at room temperature in a dark moist chamber. All sections were counterstained with haematoxylin for 20s, mounted with mounting medium and covered by a coverslip.

Lesion Scoring for Histopathological Evaluation

All variables were graded from 0 to 4 based on the percentages of observed tissue areas that included interstitial pneumonia, bronchoalveolar lesions, cellular lesions and vascular lesions. The viral antigen was evaluated from IHC, and three scores were assigned (Supplementary Table S2).

Inflammatory Mediator Determination

To inactivate SARS-CoV-2, 10X RIPA lysis buffer (Abcam, UK) was added into the homogenized lung tissues to achieve 1× concentration. The samples were incubated at room temperature for 45 min and then diluted to 1:5 ratio with DMEM media. PGE_2 and IL-6 concentrations (pg/mL) were measured in the lung tissue by using individual ELISA kits for hamster PGE_2 (MyBioSource, USA) and IL-6 (MyBioSource, USA) following the manufacturer's instructions.

Statistical Analysis

SPSS statistical software version 22.0 was used (IBM, USA). The data analysis was performed by using the Shapiro–Wilk test to determine the normality then using the one-way ANOVA or the non-parametric Kruskal–Wallis test. The data are presented as mean ± SD. All differences are considered statistically significant at p-values <0.05.

Results

SARS-CoV-2 Infection in Golden Syrian Hamsters and Tolerability of the Treatment

Hamsters were acclimatized and observed for health status before starting the experiment. Blood chemistry was collected, and the level of alanine aminotransferase and creatinine were measured to determine liver and kidney function, respectively. All animals had normal values, and no significant difference was observed among the four groups of treatment (Table 1). To test the efficacy of fingerroot extract, hamsters were infected with 3.75×10^4 PFU of SARS-CoV-2 at day 0, then the overall physical appearance and routine activity was observed at day 1 post-infection. The infected-hamsters then received treatment at day 2 post-infection according to their group and continued the treatment for 7 days (Figure 2A). Overall, hamsters could tolerate the treatments; only one hamster in the vehicle control group died at day 3 post-infection with the indication of dehydration. The data from weight monitoring after infection showed signs of weight reduction at day 2 post-infection, and significant reduction at day 3–4 post-infection in the favipiravir group (Figure 2B). Hamsters treated with fingerroot extract showed a recovery in weight reduction at day 6–8 post-infection, in a similar pattern to the vehicle control group. Overall, the weight change did not exceed 15%, which is the cut-off for a humane endpoint. All hamsters in the treatment groups were active, bright, alert and responsive (Table 1).

The Concentration of Panduratin a in Plasma and Lung Tissue

Panduratin A, as a major bioactive component in fingerroot extract, was determined in both plasma and lung tissue by LC-MS analysis, as shown in Table 2. We found that the panduratin A level in animals receiving 300 mg/kg fingerroot extract had a mean value of 2288.54 ± 1556.80 μg/L in plasma, while the panduratin A level in animals receiving

Table 1 Blood Chemistry Values and Animal Health Status of Hamsters Before the Experiment

	Vehicle Control	Finggerroot 300 mg/kg	Finggerroot 1000 mg/kg	Favipiravir 1000 mg/kg
Alanine Aminotransferase (U/L)	66.92 ± 23.14	58.42 ± 14.15	74.17 ± 36.20	71.25 ± 54.18
Creatinine (mg/dL)	0.51 ± 0.02	0.51 ± 0.02	0.57 ± 0.07	0.57 ± 0.05
Health status	One dead hamster which weight was lower than 10% of body weight at day 3 post-infection. No external wound or lesion was found.	BAR	BAR	BAR

Notes: The data are presented as mean ± SD. (n = 12 per treatment group). Reference range in hamster: Alanine aminotransferase 22–128 U/L, creatinine 0.4–1.00 mg/dL.
Abbreviations: BAR, bright alert responsive.

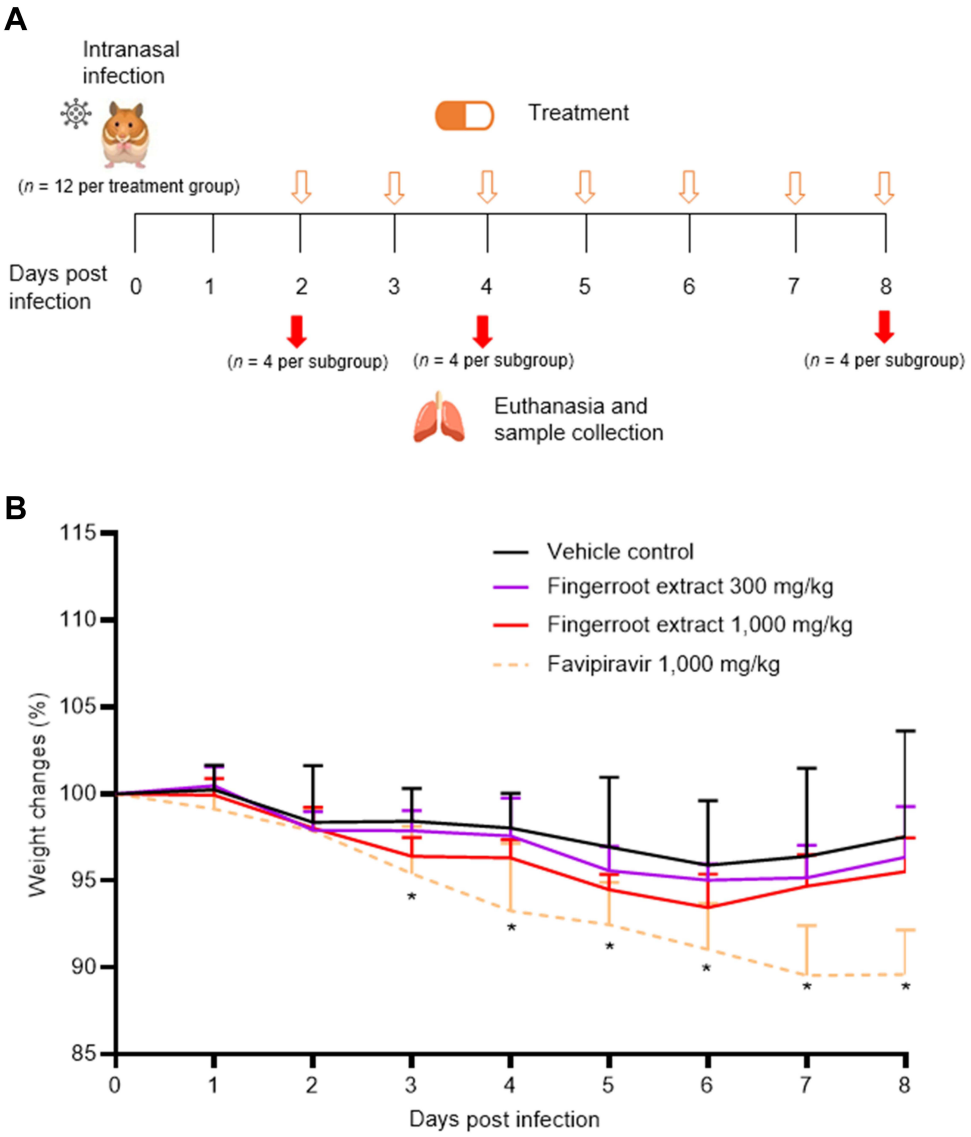

Figure 2 Animal experimental scheme and weight changes after infection and treatment. (**A**) The scheme of the animal study design (orange arrows: treatment; red arrows: euthanasia). (**B**) Weight changes in percentage, after infection and treatment (n = 12 per treatment group, 4 per subgroup). Statistical analysis was performed by using one-way ANOVA: *p < 0.05.

1000 mg/kg fingerroot extract had a mean value of 8237.59 ± 2904.74 μg/L in plasma. The average panduratin A concentrations in lung tissue were 510.25 ± 329.37 and 2015.74 ± 708.53 μg/g in the 300 and 1000 mg/kg fingerroot extract groups, respectively.

Table 2 The Concentration of Panduratin A in Plasma and Lung Tissues

	Vehicle Control	Fingerroot 300 mg/kg	Fingerroot 1000 mg/kg
Plasma (μg/L)			
Day 2	ND	2488.70 ± 2190.57	9731.30 ± 3713.65
Day 4	ND	1884.76 ± 1067.82	7288.19 ± 2566.49
Day 8	ND	2492.15 ± 1501.07	7693.27 ± 2446.99
Lung (μg/g tissue)			
Day 2	ND	541.39 ± 300.99	2247.40 ± 748.25
Day 4	ND	554.24 ± 485.91	1510.32 ± 697.78
Day 8	ND	435.13 ± 244.27	2289.50 ± 530.90

Notes: The data are presented as mean ± SD. (n = 12 per treatment group, 4 per subgroup).
Abbreviation: ND, not detected.

SARS-CoV-2 Viral Loads in Lung Tissues

To evaluate the antiviral efficacy of fingerroot extract compared to the vehicle and favipiravir in hamsters infected with SARS-CoV-2, lung tissues were obtained at day 2, 4 and 8 post-infection for quantification of viral load. SARS-CoV-2 RNA was extracted from lung tissues, and qRT-PCR was carried out to quantify the viral RNA level in the lung of SARS-CoV-2 infected hamsters. The viral RNA load in the lung tissue of each hamster in the different treatment groups was presented as RNA copies per gram of lung tissue (Figure 3A). We also determined the infectious titers in homogenized lung tissue by FFA and presented the infectious viral load as FFU per gram of lung tissue (Figure 3B). The viral RNA and infectious viral titer were high in lung tissue, at around 8 log10 copies/gram tissue and 6 log10 FFU/gram tissue at day 2 and 4 post-infection, respectively, and there was no significant difference in viral RNA and viral titer among treatment groups. However, we found that viral RNA were reduced, and viral titer were undetected at day 8 post-infection in all groups.

Histopathology of Hamster Lung Tissues

Lung specimens collected from euthanized hamsters at day 2, 4 and 8 post-infection were evaluated and scored for lung pathological changes in a blind manner, based on the severity of interstitial pneumonia, bronchiole/alveolar/cellular/vascular lesion and IHC. At day 2 post-infection, lungs from all groups showed several signs that indicated infection in the lung. The epithelial bronchioles were damaged, sloughed and proliferated, and some also formed syncytium. The

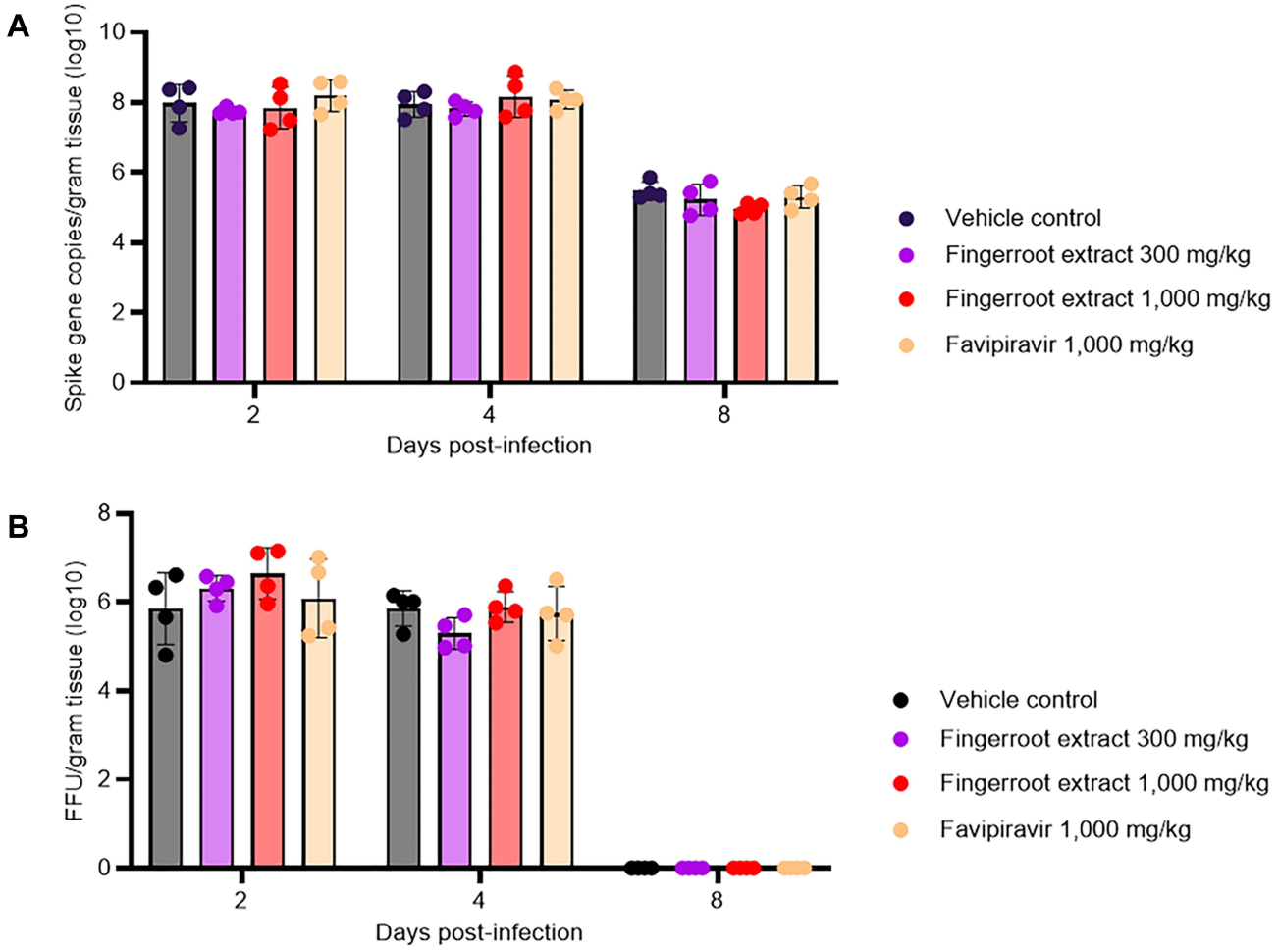

Figure 3 SARS-CoV-2 viral load in the lung tissue of infected hamsters. Lung tissues were collected from euthanized hamsters treated with vehicle control (50% DMSO), 300 mg/kg fingerroot extract, 1000 mg/kg fingerroot extract, and 1000 mg/kg favipiravir (**A**) Viral RNA levels in lung tissues were quantified by qRT-PCR and expressed as RNA copies per gram of tissue (n = 12 per treatment group, 4 per subgroup). (**B**) Viral titer by FFA presented as FFU per gram of tissue (n = 12 per treatment group, 4 per subgroup). The data are presented as mean ± SD, and dots indicate the data from individual hamsters.

pulmonary arteries showed congestion, inflammation and hemorrhage (Figure 4A). The interalveolar septa were diffused and thickened. The alveolar spaces were reduced according to the expansion of the inflammatory cell infiltration, especially mononuclear cell infiltration, and pneumocyte type 2 proliferation (Figure 4B and C). The alveolar capillaries were engorged and congested (Figure 4D). The IHC of viral antigen is moderately positive in the bronchiolar epithelium and alveolar septum. However, after treatment with fingerroot extract or favipiravir, the severity of lesions in the lung samples from either fingerroot extract or favipiravir at day 4 and 8 was reduced and exhibited an improvement in lung pathological changes compared to the vehicle control group. Next, we scored the histopathological changes of the lung tissues from each group and compared every group using the Kruskal–Wallis test (Table 3). The results showed a significant reduction of total score in the groups treated with 300 and 1000 mg/kg of fingerroot extract and 1000 mg/kg of favipiravir, with favipiravir displaying the greatest histopathological score reduction ($p < 0.001$). The subscores for interstitial pneumonia and bronchiole/alveolar/cellular/vascular lesion were also significantly reduced in the fingerroot extract and favipiravir groups compared to the vehicle control group ($p = 0.011$, < 0.001, < 0.001 and < 0.001, respectively). In contrast, the IHC score of the 1000 mg/kg of fingerroot extract and 1000 mg/kg of favipiravir groups were slightly reduced but not statistical significant ($p = 0.205$).

The Concentration of Inflammatory Mediators in Lung Tissues

The levels of PGE_2 and IL-6, as inflammatory mediators, in the lung tissues at day 4 post-infection were measured using commercial ELISA kits for hamster PGE_2 and IL-6. The results showed that PGE_2 concentrations were significantly reduced in the 1000 mg/kg of fingerroot extract and 1000 mg/kg of favipiravir groups compared to the vehicle control

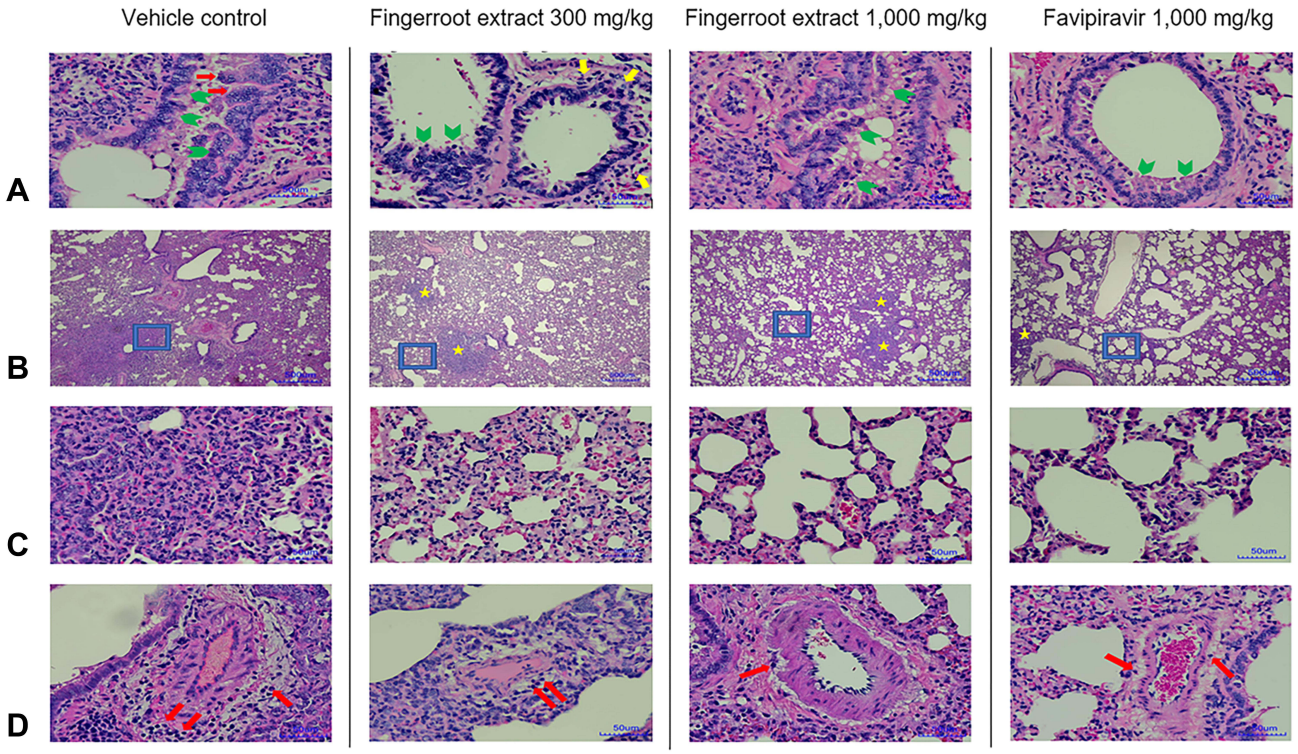

Figure 4 Histopathological changes of lung tissues at day 8 post-infection. (**A**) Representative H&E images of bronchiole lesion (Scale bars: 50 mm): epithelial bronchiole proliferation (green arrow head) with cytopathic effects and syncytium (red arrow) for vehicle control (50% DMSO), and mild peribronchial inflammation (yellow arrow) in fingerroot extract 300 and 1000 mg/kg and favipiravir 1000 mg/kg (n = 12 per treatment group, 4 per subgroup). (**B**) and (**C**) Representative H&E images of alveolar lesion: diffuse interstitial pneumonia was observed in the vehicle control (50% DMSO), multifocal interstitial pneumonia (yellow star) was observed in fingerroot extract 300 and 1000 mg/kg and favipiravir 1000 mg/kg. (**C**) Parenchyma and airway were expanded by mononuclear inflammatory cells and hyaline matrix. The severity of alveolar lesions was visually improved in fingerroot extract 300 and 1000 mg/kg and favipiravir 1000 mg/kg (n = 12 per treatment group, 4 per subgroup). (**C**) are magnifications of the blue boxes shown in (**B**) (Scale bars: 500 mm (**B**) and 50 mm (**C**)). (**D**) Representative H&E images of vascular lesions (Scale bars: 50 mm): a moderate degree of perivascular edema and mononuclear cells infiltration (red arrow) was shown in the vehicle control (50% DMSO) and fingerroot extract 300 mg/kg, while a mild degree of perivascular edema and cellular infiltration was shown in fingerroot extract 1000 mg/kg and favipiravir 1000 mg/kg (n = 12 per treatment group, 4 per subgroup).

Table 3 Histopathological Analysis Score of Lung Tissues After Treatments for 7 Days

Histopathological Analysis Score	Vehicle Control	Fingerroot 300 mg/kg	Fingerroot 1000 mg/kg	Favipiravir 1000 mg/kg	*p*-value
Interstitial pneumonia	3.73 ± 0.47	2.83 ± 0.58	3.14 ± 0.45	3.04 ± 0.89	0.011
Bronchiole and alveolar lesion	3.82 ± 0.40	2.42 ± 0.36	3.00 ± 0.50	2.17 ± 0.65	<0.001
Cellular lesions	1.00 ± 0.00	0.25 ± 0.34	0.55 ± 0.42	0.58 ± 0.47	<0.001
Vascular lesions	3.64 ± 0.50	2.13 ± 0.23	2.41 ± 0.63	1.75 ± 0.62	<0.001
Immunohistochemistry	1.64 ± 0.67	1.67 ± 0.39	1.18 ± 0.75	1.13 ± 0.91	0.205
Total score	13.82 ± 1.17	9.29 ± 0.78	10.27 ± 1.19	8.67 ± 1.76	<0.001

Notes: The data are presented as mean ± SD. (n = 12 per treatment group).

group, twofold approximately (Figure 5A). Similarly, IL-6 concentrations also approximately 1.5-fold reduced in the 1000 mg/kg of fingerroot extract and 1000 mg/kg of favipiravir groups compared to the vehicle control group (Figure 5B).

Discussion

In a previous study, our team revealed the potential of fingerroot extract and its phytochemical panduratin A as a candidate against SARS-CoV-2 in Vero E6 and Calu-3 cells.[13] However, the difficulty in purifying panduratin A from fingerroot leads to the development of fingerroot extract for phytopharmaceutical product development. Consequently, we selected a hamster model for in vivo study, to determine the efficacy of fingerroot extract against SARS-CoV-2 infection. One infected hamster death was found in the vehicle control group; however, all hamsters in the treatment groups survived throughout the experiment. This may indicate that treatment with fingerroot extract and favipiravir could reduce mortality of animals from the infection. Correspondingly, Tostanoski et al reported that 6 of 16 infected hamsters were met euthanasia criteria of more than 20% weight loss at day 6–7 post-infection.[25] A decline in

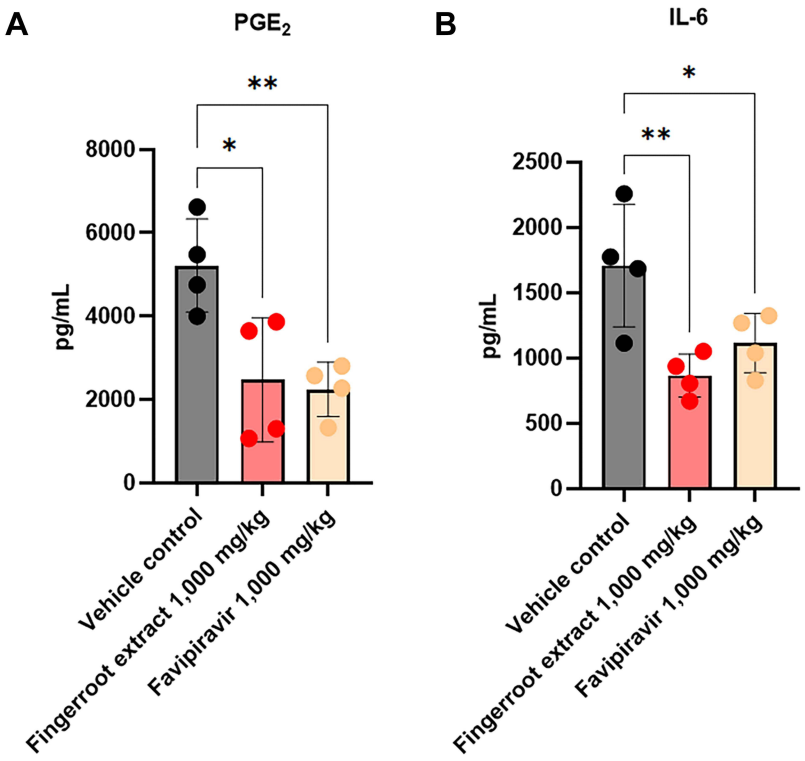

Figure 5 Inflammatory mediator concentrations in the lung tissues. Lung tissues were collected from euthanized hamsters at day 4 post-infection treated with vehicle control (50% DMSO), 1000 mg/kg fingerroot extract, and 1000 mg/kg favipiravir. (**A**) PGE_2 and (**B**) IL-6 concentrations (pg/mL) were measured in the RIPA inactivated lung homogenates using ELISA for hamster PGE_2 and IL-6. Data are presented as mean ± SD (n = 12 per treatment group, 4 per subgroup). Statistical analysis was performed by using one-way ANOVA: *p < 0.05, **p < 0.005, and ***p < 0.001.

body weight after inoculation were observed in most animals. The weight reduction from day 0 to day 2 post-infection might be caused by the infection, because every group showed a similar pattern of decline. In contrast, the difference in weight change in other groups from day 2 to day 8 post-infection indicated the effect of treatment. Other research treating infected-hamsters with favipiravir also found a prolong weight reduction.[26,27] Moreover, they found that a higher dose of favipiravir could lower the weight. According to the review report of favipiravir from Pharmaceuticals and Medical Devices Agency, Japanese FDA, an oral single-dose of greater than 500 mg/kg favipiravir caused weight loss in both mice and rats.[28] Our results show that the weight reduction in hamsters that received favipiravir was the greatest, followed by those that received 1000 and 300 mg/kg fingerroot extract, respectively. Interestingly, all animals in the fingerroot extract groups showed a recovery of weight reduction on day 6–8 post-infection, similar to the vehicle control group. Our results correspond with other safety profiles of fingerroot extract in rodents. According to Saraithong et al,[29] feeding fingerroot extract to rats for 60 days showed no significant changes in body weight, hematological and biochemical parameters, nor in the functions and histopathology of the liver and kidney. Fingerroot extract seems to be safe for tested animals with the no-observed-adverse-effect level (NOAEL) more than 240 mg/kg/day.

In our study, panduratin A levels in the plasma and lung were increased in a dose-proportional response. Fingerroot extract 1000 mg/kg could yield panduratin A levels of 7000–9000 μg/L in plasma and 1500–2500 μg/L in the lung. Kanjanasirirat et al[13] reported that panduratin A can inhibit SARS-CoV-2 in Vero E6 and Calu-3 cells, with an IC_{50} of 0.81 and 2.04 μM, respectively. Yun et al[20] found that panduratin A from 75% methanol extract of fingerroot can inhibited NO and PGE_2 production in RAW264.7 cells, with an IC_{50} of 0.175 and 0.0195 μM, respectively. Tewtrakul et al[30] also found that panduratin A from chloroform and methanol extract of fingerroot can inhibited NO and PGE_2 production, with an IC_{50} of 5.3 and 10.5 μM, respectively. These concentrations after oral administration are adequate for both antiviral and anti-inflammatory activities in vivo. However, fingerroot extract could not reduce the viral output due to the late treatment model of our study. At a late stage of treatment, the extract decreased lung inflammation and the pathophysiology of the SARS-CoV-2 infection. Further investigation into the pharmacokinetics of panduratin A and formulation development are required, in order to address the lack of full pharmacokinetic data for panduratin A in rodents and large animal species.

Viral load measurements in lung tissues were conducted on day 2, 4 and 8 post-infection. There was no effect on viral loads for any treatment, compared to the vehicle control group. On day 8 post-infection, significantly lower levels of RNA were detected in the lungs, with complete clearance of infectious virus of all treatment groups, suggesting that all infected hamsters developed immune responses and recovered. Other studies have indicated that chloroquine and hydroxychloroquine exhibited significant antiviral activities in vitro against SARS-CoV-2, but they were ineffective against SARS-CoV-2 in vivo.[31,32] Panduratin A levels in plasma and lung tissue were found to be 2–10 times higher than the IC_{50} value conducted in Calu-3 cells, at 2.04 μM.[13] Moreover, favipiravir also showed no inhibition activity on viral replication. With this finding, the main limitation in viral inhibition might be the late treatment after infection. Previous studies have reported that the SARS-CoV-2 viral load in the hamster lung peaked at day 2 post-infection and rapidly eradicated the virus at day 7 post-infection.[3,27,33] In our experiment, hamsters received the fingerroot extract treatments at day 2 post-infection, as a late treatment model, suggesting that treatments at the peak of the infection could not reduce the viral output. Our finding was in contrast with the in vivo findings in other studies, where favipiravir at high doses (1000 mg/kg) exhibited an antiviral effect in hamsters.[26,27] The source of this difference might be (i) the time to treat, 1 h before inoculation instead of day 2 post-infection in our experiment, (ii) the route of administration, intraperitoneal injection instead of oral administration in our experiment, and (iii) the age of the hamsters at the time of inoculum, 4 weeks instead of 8–10 weeks in our experiment, aged hamsters displayed notable weight loss and severe lung histopathology similar to age-dependent differences of COVID-19 patients.[34] Considering the clinical uses, our experimental designs were relevant to most COVID-19 patients, which involve late treatment with oral favipiravir. In addition, the elders are more likely to have severe COVID-19 symptoms, and favipiravir is commercially available in oral dosage form in Thailand. This finding indicated that earlier treatment of antivirals might provide better virological outcome.

Interestingly, we found a histopathological improvement of lesions in the lung tissues of the treatment groups compared to the vehicle control group. With histopathological scoring, we detected that overall inflammation and lesions were alleviated in all treatment groups. Analysis between groups showed a significant difference in the cumulative score between treatments and vehicle control, but no difference between the treatments. This demonstrated that all treatments

could ameliorate the pathology in the lung. Other studies have reported that lung inflammation of SARS-CoV-2 infected hamsters peaked at day 5 post-infection; furthermore, at day 14 post-infection, the lung viral titer was undetectable and the process of tissue regeneration had begun.[35] There are two stages of COVID-19 pathogenesis: immunosuppression and tight junction impairment in the early stage, and a cytokine storm and multiple-organ dysfunction in the late stage.[36] Inflammation is a key to disease progression in the late stage, mostly caused by IL-6 and TNF-α.[37] A recent report demonstrated that several inflammatory cytokines were up-regulated in the lungs of SARS-CoV-2-infected hamsters including IL-6, IL-1β, and TNF-α.[38] Notably, several herbs and their phytochemicals that have been found to inhibit SARS-CoV-2 also possess anti-inflammatory and immunomodulatory activities, eg, *Azadirachta indica, Withania somnifera* and glycyrrhizin.[39–41] Our finding exhibited 1.5-fold reduction of IL-6 level in lung tissues at day 4 post-infection, which is the peak level of cytokines in the lung of infected hamsters.[42] Another inflammatory mediator that is considered important to be related to disease progression is PGE_2. The increased level of PGE_2 in the plasma of COVID-19 patients associated with disease severity, due to its immunosuppressive effect and the disruption of the immune response.[43,44] Interestingly, our finding exhibited twofold reduction of PGE_2 level in lung tissues at day 4 post-infection. Thus, fingerroot extract could suppress inflammatory cytokine production in the infected hamsters. These results suggest that fingerroot extract might possess some anti-inflammatory effects, using a single mechanism or combination of mechanisms that lessen the inflammation of lung tissue in hamsters, which could reduce complications form SARS-CoV-2 infection.

Conclusion

This experiment exhibits the potential of fingerroot extract in SARS-CoV-2-infected hamsters by reduction of lung pathology and inflammatory cytokines. Fingerroot extract might be useful as complementary medicines in terms of anti-inflammatory to minimize long-term complications of COVID-19 infection. Further study in long-term safety, drug–herb interaction, and its pharmacokinetic/pharmacodynamic interactions should be conducted in order to maximize benefit/risk before entry into clinical development.

Abbreviations

Calu-3 cells, lung adenocarcinoma epithelial cells from human; COVID-19, coronavirus disease 2019; DMEM, Dulbecco's modified Eagle's medium; DMSO, dimethyl sulfoxide; FBS, fetal bovine serum; FFA, focus forming assay; FFPE, formalin-fixed paraffin-embedded; H&E, hematoxylin and eosin; IC_{50}, inhibitory concentration; IHS, immunohistochemistry; IL-6, interleukin-6; NO, nitric oxide; PBS, phosphate buffered saline; PFU, plaque-forming unit; PGE_2, prostaglandin E2; SARS-CoV-2, severe acute respiratory syndrome coronavirus 2; TNF-α, tumor necrosis factor-α; Vero E6 cells, kidney epithelial cells of *Cercopithecus aethiops*.

Data Sharing Statement

The data that support the findings of this study are available from the corresponding author upon reasonable request. Some data may not be made available because of privacy or ethical restrictions.

Ethics Approval

The animal study protocol was approved by the Faculty of Veterinary Science, Mahidol University-Institute Animal Care and Use Committee (approval no. MUVS-2020-07-26; approval date Oct 01, 2020).

Acknowledgments

We express gratitude to the Excellence Centre for Drug Discovery for providing fingerroot extract. We express our utmost gratitude to the Ministry of Public Health, Thailand, for providing favipiravir.

Author Contributions

All authors made a significant contribution to the work reported, whether that is in the conception, study design, execution, acquisition of data, analysis and interpretation, or in all these areas; took part in drafting, revising or critically

reviewing the article; gave final approval of the version to be published; have agreed on the journal to which the article has been submitted; and agree to be accountable for all aspects of the work.

Funding

This work was supported by the Faculty of Medicine Ramathibodi Hospital, Mahidol University (CF63010 to Somchai Chutipongtanate and Phisit Khemawoot), the National Research Council of Thailand (to Suradej Hongeng) and the 60th Year Supreme Reign of His Majesty King Bhumibol Adulyadej Scholarship, Mahidol University (to Teetat Kongratanapasert). This project is supported by Mahidol University (Reinventing University Program), and the Office of National Higher Education Science Research and Innovation Policy Council (B17F640004 to Somchai Chutipongtanate).

Disclosure

The authors declare no conflicts of interest.

References

1. World Health Organization. COVID-19 Clinical management: living guidance; 2021. Available from: https://www.who.int/publications/i/item/WHO-2019-nCoV-clinical-2021-1. Accessed January 09, 2023.
2. Centers for Disease Control and Prevention. Symptoms of COVID-19; 2021. Available from: https://www.cdc.gov/coronavirus/2019-ncov/symptoms-testing/symptoms.html. Accessed January 9, 2023.
3. Mason RJ. Pathogenesis of COVID-19 from a cell biology perspective. *Eur Respir J*. 2020;55(4):2000607. doi:10.1183/13993003.00607-2020
4. National Institutes of Health. Therapeutic management of adults with COVID-19; 2021. Available from: https://www.covid19treatmentguidelines.nih.gov/therapeutic-management/. Accessed January 9, 2023.
5. Department of Medical Services. Guidelines on clinical practice, diagnosis, treatment, and prevention of healthcare-associated infection for COVID-19; 2021. Available from: https://ddc.moph.go.th/viralpneumonia/eng/guideline_hcw.php. Accessed January 09, 2023.
6. The RECOVERY Collaborative Group. Dexamethasone in hospitalized patients with COVID-19. *N Engl J Med*. 2020;384(8):693–704.
7. Beigel JH, Tomashek KM, Dodd LE, et al. Remdesivir for the treatment of COVID-19 — final report. *N Engl J Med*. 2020;383(19):1813–1826.
8. Jayk Bernal A, Gomes da Silva MM, Musungaie DB, et al. Molnupiravir for oral treatment of COVID-19 in nonhospitalized patients. *N Engl J Med*. 2022;386(6):509–520.
9. Hammond J, Leister-Tebbe H, Gardner A, et al. Oral nirmatrelvir for high-risk, nonhospitalized adults with COVID-19. *N Engl J Med*. 2022;386(15):1397–1408.
10. Vacharathit V, Aiewsakun P, Manopwisedjaroen S, et al. CoronaVac induces lower neutralising activity against variants of concern than natural infection. *Lancet Infect Dis*. 2021;21(10):1352–1354. doi:10.1016/S1473-3099(21)00568-5
11. Atanasov AG, Zotchev SB, Dirsch VM, et al. Natural products in drug discovery: advances and opportunities. *Nat Rev Drug Discov*. 2021;20(3):200–216. doi:10.1038/s41573-020-00114-z
12. Sa-Ngiamsuntorn K, Suksatu A, Pewkliang Y, et al. Anti-SARS-CoV-2 activity of *Andrographis paniculata* extract and its major component andrographolide in human lung epithelial cells and cytotoxicity evaluation in major organ cell representatives. *J Nat Prod*. 2021;84:1261–1270. doi:10.1021/acs.jnatprod.0c01324
13. Kanjanasirirat P, Suksatu A, Manopwisedjaroen S, et al. High-content screening of Thai medicinal plants reveals *Boesenbergia rotunda* extract and its component Panduratin A as anti-SARS-CoV-2 agents. *Sci Rep*. 2020;10(1):19963. doi:10.1038/s41598-020-77003-3
14. Hoffmann M, Kleine-Weber H, Schroeder S, et al. SARS-CoV-2 cell entry depends on ACE2 and TMPRSS2 and is blocked by a clinically proven protease inhibitor. *Cell*. 2020;181(2):271–280. doi:10.1016/j.cell.2020.02.052
15. Imai M, Iwatsuki-Horimoto K, Hatta M, et al. Syrian hamsters as a small animal model for SARS-CoV-2 infection and countermeasure development. *PNAS*. 2020;117(28):16587–16595. doi:10.1073/pnas.2009799117
16. Eng-Chong T, Yean-Kee L, Chin-Fei C, et al. *Boesenbergia rotunda*: from ethnomedicine to drug discovery. *eCAM*. 2012;2012:473637. doi:10.1155/2012/473637
17. Ongwisespaiboon O, Jiraungkoorskul W. Fingerroot, *Boesenbergia rotunda* and its aphrodisiac activity. *Pharmacogn Rev*. 2017;11(21):27–30. doi:10.4103/phrev.phrev_50_16
18. National Center for Biotechnology Information. PubChem compound summary for CID 6483648; 2021. Available from: https://pubchem.ncbi.nlm.nih.gov/compound/Panduratin-A. Accessed January 9, 2023.
19. Cheenpracha S, Karalai C, Ponglimanont C, Subhadhirasakul S, Tewtrakul S. Anti-HIV-1 protease activity of compounds from Boesenbergia pandurata. *Bioorg Med Chem*. 2006;14(6):1710–1714. doi:10.1016/j.bmc.2005.10.019
20. Yun J-M, Kwon H, Hwang J-K. *In vitro* anti-inflammatory activity of panduratin A isolated from *Kaempferia pandurata* in RAW264.7 cells. *Planta Med*. 2003;69(12):1102–1108.
21. Mohan S, Hobani YH, Shaheen E, et al. Ameliorative effect of Boesenbergin A, a chalcone isolated from *Boesenbergia rotunda* (Fingerroot) on oxidative stress and inflammation in ethanol-induced gastric ulcer *in vivo*. *J Ethnopharmacol*. 2020;261:113104. doi:10.1016/j.jep.2020.113104
22. Santa Cruz A, Mendes-Frias A, Oliveira AI, et al. Interleukin-6 is a biomarker for the development of fatal severe acute respiratory syndrome coronavirus 2 pneumonia. *Front Immunol*. 2021;12:613422. doi:10.3389/fimmu.2021.613422
23. The Royal Thai Government Gazette. Announcement of the use to animals for scientific work committee: ethics of use to animals for scientific work; 2016:21–25.

24. Talbot SR, Biernot S, Bleich A, et al. Defining body-weight reduction as a humane endpoint: a critical appraisal. *Lab Anim*. 2020;54(1):99–110. doi:10.1177/0023677219883319
25. Tostanoski LH, Wegmann F, Martinot AJ, et al. Ad26 vaccine protects against SARS-CoV-2 severe clinical disease in hamsters. *Nat Med*. 2020;26 (11):1694–1700. doi:10.1038/s41591-020-1070-6
26. Kaptein SJF, Jacobs S, Langendries L, et al. Favipiravir at high doses has potent antiviral activity in SARS-CoV-2-infected hamsters, whereas hydroxychloroquine lacks activity. *PNAS*. 2020;117(43):26955–26965. doi:10.1073/pnas.2014441117
27. Driouich J-S, Cochin M, Lingas G, et al. Favipiravir antiviral efficacy against SARS-CoV-2 in a hamster model. *Nat Commun*. 2021;12(1):1735. doi:10.1038/s41467-021-21992-w
28. Pharmaceuticals and Medical Devices Agency. Review report of Avigan(favipiravir); 2014. Available from: https://www.pmda.go.jp/files/000210319.pdf. Accessed January 9, 2023.
29. Saraithong P, Saenphet S, Saenphet K. Safety evaluation of ethanol extracts from *Boesenbergia rotunda* (L). Mansf. in male rats. *Trends Res Sci Technol*. 2010;2(1):19–22.
30. Tewtrakul S, Subhadhirasakul S, Karalai C, Ponglimanont C, Cheenpracha S. Anti-inflammatory effects of compounds from *Kaempferia parviflora* and *Boesenbergia pandurata*. *Food Chem*. 2009;115(2):534–538. doi:10.1016/j.foodchem.2008.12.057
31. Rosenke K, Jarvis MA, Feldmann F, et al. Hydroxychloroquine prophylaxis and treatment is ineffective in macaque and hamster SARS-CoV-2 disease models. *JCI Insight*. 2020;5(23):e143174. doi:10.1172/jci.insight.143174
32. Weston S, Coleman CM, Haupt R, et al. Broad anti-coronavirus activity of food and drug administration-approved drugs against SARS-CoV-2 *in vitro* and SARS-CoV *in vivo*. *J Virol*. 2020;94(21):e01218–01220. doi:10.1128/JVI.01218-20
33. Sia SF, Yan LM, Chin AWH, et al. Pathogenesis and transmission of SARS-CoV-2 in golden hamsters. *Nature*. 2020;583(7818):834–838. doi:10.1038/s41586-020-2342-5
34. Osterrieder N, Bertzbach LD, Dietert K, et al. Age-dependent progression of SARS-CoV-2 infection in Syrian hamsters. *Viruses*. 2020;12(7):779. doi:10.3390/v12070779
35. Nouailles G, Wyler E, Pennitz P, et al. Temporal omics analysis in Syrian hamsters unravel cellular effector responses to moderate COVID-19. *Nat Commun*. 2021;12(1):4869. doi:10.1038/s41467-021-25030-7
36. Tian W, Zhang N, Jin R, et al. Immune suppression in the early stage of COVID-19 disease. *Nat Commun*. 2020;11(1):5859. doi:10.1038/s41467-020-19706-9
37. Samprathi M, Jayashree M. Biomarkers in COVID-19: an up-to-date review. *Front Pediatr*. 2021;8(972):607647. doi:10.3389/fped.2020.607647
38. Francis ME, Goncin U, Kroeker A, et al. SARS-CoV-2 infection in the Syrian hamster model causes inflammation as well as type I interferon dysregulation in both respiratory and non-respiratory tissues including the heart and kidney. *PLoS Pathog*. 2021;17(7):e1009705. doi:10.1371/journal.ppat.1009705
39. Matveeva T, Khafizova G, Sokornova S. In search of herbal anti-SARS-CoV2 compounds. *Front Plant Sci*. 2020;11(1807):589998. doi:10.3389/fpls.2020.589998
40. Murck H. Symptomatic protective action of glycyrrhizin (licorice) in COVID-19 infection? *Front Immunol*. 2020;11(1239):1239. doi:10.3389/fimmu.2020.01239
41. Lim XY, Teh BP, Tan TYC. Medicinal plants in COVID-19: potential and limitations. *Front Pharmacol*. 2021;12(355):611408.
42. Chan JF-W, Zhang AJ, Yuan S, et al. Simulation of the clinical and pathological manifestations of coronavirus disease 2019 (COVID-19) in a golden Syrian hamster model: implications for disease pathogenesis and transmissibility. *Clin Infect Dis*. 2020;71(9):2428–2446.
43. Ricke-Hoch M, Stelling E, Lasswitz L, et al. Impaired immune response mediated by prostaglandin E2 promotes severe COVID-19 disease. *PLoS One*. 2021;16(8):e0255335.
44. Park Y-J, Acosta D, Vassell R, et al. D-dimer and CoV-2 spike-immune complexes contribute to the production of PGE2 and proinflammatory cytokines in monocytes. *PLoS Pathog*. 2022;18(4):e1010468.